analytical chemistry

Article

pubs.acs.org/ac

Magnetic Nanoparticle-Based Platform for Characterization of Histidine-Rich Proteins and Peptides

Shin-Yi Huang and Yu-Chie Chen*

Department of Applied Chemistry, National Chiao Tung University, Hsinchu 300, Taiwan

Supporting Information

ABSTRACT: In this study, we developed a platform that can be used to rapidly enrich polyhistidine(His)-tagged proteins/peptides from complex samples selectively using the Fe_3O_4@Al_2O_3 magnetic nanoparticles (MNPs) as the affinity probes. At pH 7, the dissociation constant between poly-His, i.e., His_6, and the Fe_3O_4@Al_2O_3 MNPs was ~10^{-5} M and the trapping capacity was ~100 nmol/mg for His_6. Enrichment was achieved by vigorously mixing the sample solution (<2 μL) and the MNPs (1−3 μg) by pipetting directly onto a matrix-assisted laser desorption/ionization (MALDI) plate for 10 s. The time for the enrichment and the sample volume required for analysis are therefore greatly reduced. After enrichment, the MNP−target species conjugates were promptly isolated by positioning a magnet on the edge of the sample well to aggregate the conjugates into a small spot within ~5 s so that the nontarget species could be easily removed. Additionally, the problem of finding "sweet spots" on the target species during the MALDI mass spectrometry (MS) analysis was greatly reduced by magnetically isolating the target species on the MALDI plate. The limit of detection for His_6 was, therefore, as low as ~400 amol. His_6 and AHHAHHAAD AHHAHHAAD spiked in a protein digest and in human plasma, respectively, were used as the samples to demonstrate the practicability of this approach in selective enrichment of His-rich peptides from complex samples. We also characterized His_6-tagged proteins enriched on-plate by the Fe_3O_4@Al_2O_3 MNPs followed by on-plate tryptic digestion, selective enrichment, and MALDI-MS analysis. This approach can be used to determine quickly whether His_6-tagged species are present in a sample. In addition, cell lysates containing recombinant Shiga-like toxins tagged with His_6 were used as the samples to further demonstrate that the feasibility of this approach in analyzing very complex samples. The entire analysis process, including the on-plate enrichment and enzymatic digestion followed by MALDI-MS analysis, can be completed within 10 min.

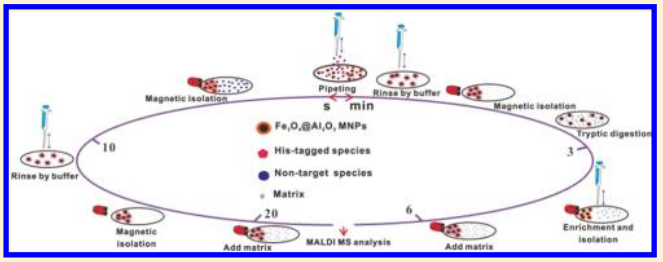

Histidine (His)-rich proteins are characteristic biomolecules that play important roles in various aspects. For example, *Plasmodium falciparum* His-rich protein 2 (HRP-II) has been recognized as a biomarker associated with malaria.[1,2] Directly detecting the biomarker from biological samples is helpful in the diagnosis of malaria. Additionally, recombinant proteins tagged with poly-His are commonly designed to isolate target species easily after protein expression from complex cell lysates.[3] These proteins are generally present in complex samples; thus, a sample pretreatment must be conducted prior to protein identification. Affinity-based analytical methods, such as immobilized metal ion affinity chromatography (IMAC)[4−21] and metal oxide affinity chromatography (MOAC),[22−41] have been developed to concentrate specific target species, such as poly-His-tagged proteins and phosphorylated species. The main concerns of using IMAC in selective enrichment of target species are metal leakage and metal toxicity.[42,43] Metal oxides are covalently bound to MOAC adsorbents; thus, the coating is relatively stable. Therefore, MOAC can provide reproducible results with better selectivity for target analytes.[39] In using magnetic nanoparticles (MNPs) coated with metal oxide to probe target species, the MNP−target species conjugates are immediately isolated from the sample solution by employing an external magnetic field. Using MNP-based MOAC as affinity probes has several advantages, including a high trapping capacity due to their high surface to volume ratio and ease of isolation owing to their magnetic property. Thus, various types of MNP-based MOAC have been explored in the past decade.[29−41] Most of the MOAC applications have been directed toward the enrichment of phosphorylated species.[29−39] His-rich species are usually enriched by Ni(II)/Cu(II) IMAC methods.[4,7,9,16,17,20,21] MNP-based MOAC can be an alternative method of selectively enriching His-rich species, considering its good metal oxide-coating stability and good selectivity toward its target species.[39] According to hard and soft acids and bases (HSAB) theory,[44] alumina-based MOAC is expected to be suitable for enriching His-rich species because Al(III) and amine are hard acids and hard bases, respectively. Alumina-MOAC has been demonstrated as effective affinity probe for concentrating phosphorylated species.[29−39] Alumina chelating with phosphate groups is mainly based on the electron-rich phosphate group. Histidine is also an electron-rich species that can chelate with an Al metal center,[45] according to HSAB

Received: January 2, 2013
Accepted: February 22, 2013
Published: March 11, 2013

theory. Thus, the alumina-MOAC is used to enrich His-rich molecules from complex samples selectively. Alumina-coated iron oxide MNPs (Fe_3O_4@Al_2O_3 MNPs) were used as the affinity probes for His-rich species in this study to isolate His-rich peptides/proteins easily. The binding constant between the Fe_3O_4@Al_2O_3 MNPs and $(His)_6$ was first investigated, and the capacity of the MNPs toward His-rich proteins/peptides was examined. Matrix-assisted laser desorption/ionization mass spectrometry (MALDI-MS) was used to confirm the results. Although the Fe_3O_4@Al_2O_3 MNPs have been previously used as effective affinity probes for phosphorylated species at low-pH conditions,[30] we herein demonstrate that the Fe_3O_4@Al_2O_3 MNPs exhibit better selectivity for His-rich proteins/peptides than phosphorylated species at neutral pH.

EXPERIMENTAL SECTION

Reagents and Materials. Tris(hydroxymethyl)-aminomethane (Tris), hydrochloric acid (36.5%), and iron(II) chloride were purchased from J.T. Baker (Phillipsburg, NJ, U.S.A.). Iron(III) chloride, aluminum isopropoxide, trypsin (from bovine pancreas), β-casein, His-tagged ubiquitin, sinapinic acid, myoglobin (from horse heart), cytochrome *c* (from bovine heart), 2,5-dihydroxylbenzoic acid (2,5-DHB), ammonium hydroxide, isopropyl β-D-1-thiogalactopyranoside (IPTG), kanamycin, human plasma, and α-cyano-4-hydroxycinnamic acid (CHCA) were purchased from Sigma-Aldrich (St. Louis, MO, U.S.A.). Acetonitrile (99%) was obtained from Merck (Darmstadt, Germany), and Luria−Bertani broth (LB broth) consisting of tryptone, yeast extract, and sodium chloride (2:1:2, w/w/w) was purchased from Becton Dickinson (Franklin Lakes, NJ, U.S.A.). Trifluoroacetic acid (99%) and phosphoric acid (85%) were obtained from Riedel−de Haen (Buchs, St. Gallen, Switzerland). His_6 was obtained from GL Biochem (Shanghai, China). Tetraethyl orthosilicate (TEOS) was obtained from Fluka (Buchs, St. Gallen, Switzerland). Millex FG 22 filters (pore size: 0.22 μm) were obtained from Merck Millipore (Billerica, MA, U.S.A.). Pall Acrodisc syringe filters with Supor membrane Pall-4612 (pore size: 0.2 μm) were obtained from Voigt Global Distribution (Lawrence, KS, U.S.A.).

Generation of Fe_3O_4@Al_2O_3 MNPs. Fe_3O_4 MNPs were first generated in an aqueous solution by the coprecipitation of Fe(III) and Fe(II) with aqueous ammonia. Iron(II) chloride (0.49 g) and iron(III) chloride (0.65 g) were dissolved in a flask containing deionized water (25 mL). The final concentration for both iron(II) chloride and iron(III) chloride in the solution was 0.1 M. Subsequently, the mixture and aqueous ammonia (33%, 25 mL) were simultaneously injected into a double-neck flask with two syringes operated by two syringe pumps at the same flow rate of 0.6 mL/min while stirring. After completing the injection, the reaction mixture was continuously stirred at room temperature for another 1 h. The generated Fe_3O_4 MNPs were separated from the resulting solution by an external magnet. The remaining MNPs were rinsed with deionized water (20 mL × 3) and ethanol (20 mL × 2). The Fe_3O_4 MNPs were stored in ethanol. Supporting Information Figure S1A shows the TEM image of the generated MNPs. The particle size was ∼18 nm.

The Fe_3O_4 MNPs were further coated with SiO_2 using TEOS as the precursor. The Fe_3O_4 MNPs (1 g) were suspended in a solvent composed of ethanol (32 mL) and deionized water (8 mL) under nitrogen-protected condition. TEOS (2 mL) was injected into the MNP suspension in an ultrasonicator (frequency: 40 Hz) for 10 min, followed by an injection of aqueous ammonia (10%, 2 mL) under sonication for another 10 min. The mixture was continuously reacted at 40 °C while stirring. After 12 h, the generated Fe_3O_4@SiO_2 MNPs were rinsed with deionized water (20 mL × 3) and methanol (20 mL × 2). The MNPs were stored in methanol (40 mL). Supporting Information Figure S1B shows the TEM image of the generated MNPs. A layer coating the surface of the MNPs is visible. As a result, the particle size (∼30 nm) of the generated MNPs became larger than that prior to SiO_2 coating.

The Fe_3O_4@SiO_2 MNPs (0.2 g) obtained above were then suspended in deionized water (40 mL) under sonication for 20 min. Aluminum isopropoxide (7.5 mg) was added to the suspension, followed by sonication for 30 min at room temperature. The mixture was placed in a reaction vial and then reacted at 80 °C in an oil bath with vigorous stirring for 1 h. The vial was moved to an ultrasonicator and was sonicated every 15 min for 1 h to suspend the MNPs thoroughly in the solution. Subsequently, the mixture was stirred at 90 °C for 30 min, uncovered to remove the generated gas, namely, 2-propanol, and then continuously stirred at 90 °C for another 2 h, covered with a loosely screwed cap. After the mixture was cooled to room temperature, the generated MNPs were isolated, rinsed with water (40 mL × 3), resuspended in deionized water, and kept until use. Supporting Information Figure S1C shows the TEM image of the generated MNPs. A layer coated on the surface of the MNPs can be seen. The particle size of the Fe_3O_4@Al_2O_3 was ∼42 nm.

Preparation of Cell Lysates. *Escherichia coli* BL21, which expresses His-tag fusion verotoxin type 2B,[46] was cultured in an LB broth (25 mg/mL, 10 mL) containing kanamycin (30 μg/mL) at 37 °C for ∼4 h. The bacterial strain was kindly provided by Professor Hiroshi Morie. When the optical density (OD) at a wavelength of 600 nm ($OD_{600\ nm}$) of the cultured bacteria became >0.3, IPTG (2.38 mg) was added to the bacterial suspension. The final IPTG concentration in the bacterial suspension was 1 mM. The bacterial sample was incubated for another 24 h. The resultant bacterial sample was centrifuged at 4000 rpm for 5 min. The supernatant was removed, and deionized water was added to the sample tube to obtain a final volume of 10 mL. The washing procedure was repeated twice. Urea (8 M, 1 mL) was added to the rinsed bacterial pellets. The mixture was then incubated at 37 °C for 2 h. The resultant cell lysate was centrifuged at 6000 rpm for 5 min. The supernatant was filtered through a filter (pore size: 0.2 m). The filtered solution containing His_6-tagged proteins was stored in a freezer (−20 °C) until use.

In-Vial Enrichment. We initially conducted the enrichment of His_6-tagged species in a centrifuge tube. The generated Fe_3O_4@Al_2O_3 MNPs (20 μg) were vortex-mixed with a sample solution (20 μL) prepared in Tris buffer (pH 7, 10 mM) in the tube for 30 min. The MNP−target species conjugates were isolated by placing an external magnet (5000 G) on the wall of the tube and then removing the supernatant. After rinsing with Tris buffer (50 μL × 3), the resulting conjugates were mixed with a MALDI matrix, namely, sinapinic acid (20 mg/mL, 1 μL). The supernatant was deposited on a MALDI plate. After solvent evaporation, the sample was ready for MALDI-MS analysis.

On-Plate Enrichment. Alternatively, we conducted the enrichment of His_6-tagged species on a MALDI plate. The Fe_3O_4@Al_2O_3 MNPs (1 μg) were mixed with a sample solution (1 or 1.5 μL) for 10 s. The MNP−target species conjugates

dx.doi.org/10.1021/ac4000128 | Anal. Chem. 2013, 85, 3347−3354

were aggregated by employing a magnet on the edge of the sample well to facilitate supernatant removal. The supernatant was taken to the other sample well for MALDI-MS analysis. The remaining conjugates were rinsed twice with Tris buffer (pH 7, 10 mM, 2 μL) on the plate. During the rinse step, the magnet was removed. A MALDI matrix, that is, 2,5-DHB (15 mg/mL, 1 μL) prepared in acetonitrile/deionized water (2:1, v/v) containing 1% phosphoric acid, was mixed with the conjugates. The magnet was then put next to the sample well to aggregate the conjugates on the edge of the well. After solvent evaporation, the sample was ready for the MALDI-MS analysis.

On-Plate Tryptic Digestion and Enrichment. The Fe_3O_4@Al_2O_3 MNPs were initially prepared in Tris buffer (pH 7, 10 mM). The Fe_3O_4@Al_2O_3 MNPs (1 μg) were mixed with a sample solution (1.5 μL) prepared in Tris buffer (pH 7, 10 mM) for 10 s. The MNP−target species conjugates were aggregated by employing a magnet on the edge of the sample well and removing the supernatant with a pipet. The conjugates were rinsed twice with Tris buffer (pH 7, 10 mM, 2 μL) on the plate. During the rinse step, the magnet was removed. Trypsin (18.75 μg/mL, 2 μL) prepared in ammonium bicarbonate buffer (20 mM, pH 8) was added to the isolated conjugates, and tryptic digestion was conducted at room temperature for 5 min. The target species were enriched with the Fe_3O_4@Al_2O_3 MNPs by pipetting the suspension in and out of the tip for 5−10 s on the plate, followed by magnetic isolation The supernatant was deposited onto the other sample well and mixed with CHCA (15 mg/mL, 1 μL) prepared in acetonitrile/deionized water for MALDI-MS analysis. The remaining MNP−target species conjugates were rinsed with deionized water (2 μL) and magnetically isolated on the edge of the sample well. The supernatant was removed. A MALDI matrix, that is, CHCA (15 mg/mL, 1 μL) prepared in acetonitrile/deionized water (2:1, v/v) containing 1% phosphoric acid, was mixed with the conjugates. The magnet was then put next to the sample well to aggregate the conjugates on the edge of the well. After solvent evaporation, the sample was ready for the MALDI-MS analysis.

Mass Spectrometry. The AutoFlex III MALDI time-of-flight MS from Bruker Daltonics (Bremen, Germany) equipped with a solid-state laser (λ = 355 nm) was used for the MS analysis. The positive-ion mode was used with the following settings: ion source 1, 19.05 kV; ion source 2, 16.59 kV; lens, 8.77 kV. The mass range was set to 4000−25 000 when the linear mode was operated. The laser focus was set to "medium" (60−70 μm), and 1000 shots were fired at each sample spot at the preset frequency of 50 Hz. When the reflectron mode was operated, the reflector and reflector 2 were set to 21.05 and 9.73 kV, respectively. The mass range was set to 800−3500, and the suppression threshold was set to 800.

RESULTS AND DISCUSSION

To confirm the generation of the Fe_3O_4@Al_2O_3 MNPs, the generated Fe_3O_4 MNPs, Fe_3O_4@SiO_2 MNPs, and Fe_3O_4@Al_2O_3 MNPs were characterized by direct laser desorption (LD) MS. We previously have demonstrated that Fe_3O_4 MNPs are efficient assisting materials for facilitating desorption/ionization processes in MS analysis.[47] Thus, direct characterizing the surface of the MNPs using direct LD MS is feasible. Parts A−C of Supporting Information Figure S2 show the direct LD mass spectra of Fe_3O_4 MNPs, Fe_3O_4@SiO_2 MNPs, and Fe_3O_4@Al_2O_3, respectively. The peak at m/z 215, corresponding to $Fe_3O_3^+$,[48] appears in all the LD mass spectra in Supporting Information Figure S2. The peak at m/z 104, corresponding to $Si_2O_3^+$,[49] appeared in the mass spectrum of Fe_3O_4@SiO_2 MNPs (Supporting Information Figure S2B) after a thin layer of silica coating on the surface of the Fe_3O_4 MNPs. After one more layer of alumina coating on the surface of the Fe_3O_4@SiO_2 MNPs, the peak at m/z 104 disappeared, but the peak at m/z 102 representing $Al_2O_3^{+50}$ appeared in the LD mass spectrum of Fe_3O_4@Al_2O_3 MNPs (Supporting Information Figure S2C). The results indicate that the Fe_3O_4@Al_2O_3 MNPs were successfully generated.

We then investigated the affinity of the Fe_3O_4@Al_2O_3 MNPs toward His_6. We found that His_6 could barely bond with the Fe_3O_4@Al_2O_3 MNPs in an acidic solution but had significant binding interactions with the MNPs at neutral pH. Supporting Information Figure S3 shows the Langmuir adsorption plot obtained from the binding behavior of the Fe_3O_4@Al_2O_3 MNPs toward His_6 at pH 7. According to this plot, the binding capacity was ∼100 nmol/mg and the dissociation constant (k_d) was $\sim 10^{-5}$ M. The results indicated the possibility of using the Fe_3O_4@Al_2O_3 MNPs as affinity probes for His_6-tagged species. The k_d is comparable with that of Cu(II)-IMAC,[42] but it is higher than that of Ni(II)-IMAC.[51] We then examined the selectivity of the Fe_3O_4@Al_2O_3 MNPs for His_6-tagged proteins. Parts A and B of Figure 1 display the

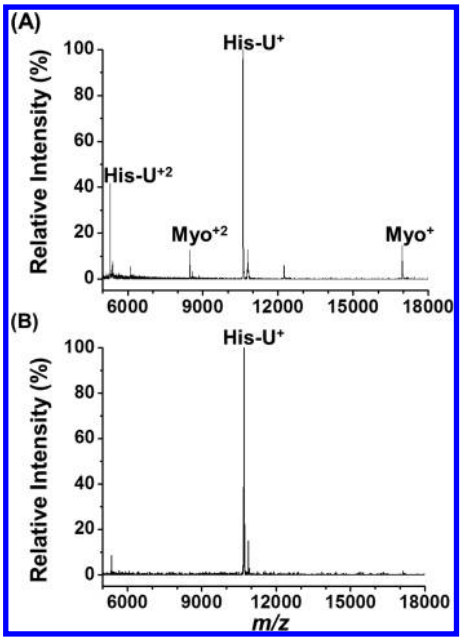

Figure 1. MALDI mass spectra obtained (A) before and (B) after using the Fe_3O_4@Al_2O_3 MNPs (20 μg) to enrich the target species from the sample solution (20 μL) containing myoglobin (Myo; 10^{-6} M) and His_6-tagged ubiquitin (His-U; 5×10^{-7} M).

MALDI mass spectra obtained before and after using the MNPs as affinity probes (20 μg), respectively, to enrich selectively the target species from a sample solution (20 μL) containing myoglobin (1 μM) and His_6-tagged ubiquitin (0.5 μM). The singly charged and doubly charged ions of myoglobin and His_6-tagged ubiquitin were observed in the mass spectrum before enrichment (Figure 1A). After enrichment, the ion peak derived from His_6-tagged ubiquitin dominated the MALDI mass spectrum (Figure 1B), whereas the ion peaks derived from myoglobin were not observed in the same mass spectrum. These results indicated that the Fe_3O_4@Al_2O_3 MNPs have the

dx.doi.org/10.1021/ac4000128 | Anal. Chem. 2013, 85, 3347−3354

capability to trap His_6-tagged proteins from a protein mixture selectively.

We performed the selective enrichment of the target species from a peptide mixture (1 μL) containing angiotensin I (10^{-7} M) and His_6 (8×10^{-8} M) using the Fe_3O_4@Al_2O_3 MNPs (1 μg) as affinity probes on a MALDI plate to shorten the time and reduce the sample volume required for analysis. Taking advantage of the magnetic property of the MNPs, an on-plate magnetic enrichment was conducted by pipetting the mixture of the MNPs and sample solution on the MALDI plate, followed by performing a magnetic isolation and then rinsing. The entire enrichment process was completed within 1 min. Parts A and B of Figure 2 present the MALDI mass spectra

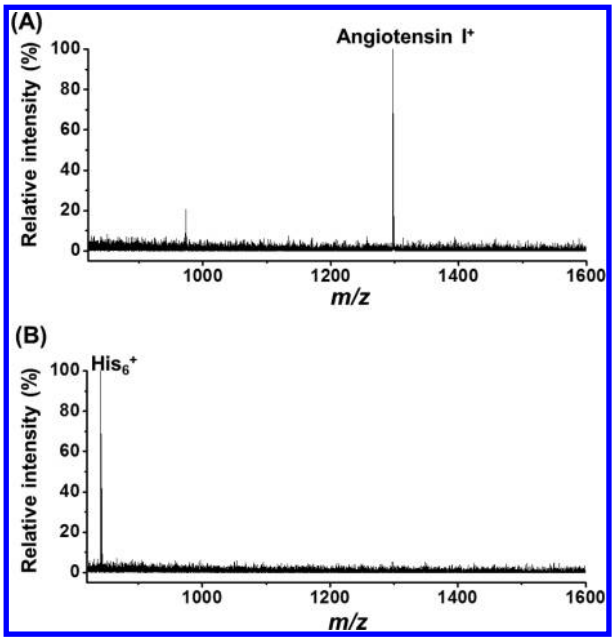

Figure 2. MALDI mass spectra obtained (A) before and (B) after using the Fe_3O_4@Al_2O_3 MNPs (1 μg) to enrich the target species from the sample solution (1 μL) containing His_6 (8×10^{-8} M) and angiotensin I (10^{-7} M).

obtained before and after using the Fe_3O_4@Al_2O_3 MNPs as affinity probes, respectively, to enrich selectively the target species from the peptide mixture on the MALDI target. Only the peak derived from angiotensin I at m/z 1296.7 appeared in the mass spectrum before enrichment (Figure 2A). However, after on-target enrichment, the peak derived from His_6 at m/z 841.3 dominated the mass spectrum and the peak at m/z 1296.7 disappeared (Figure 2B). The results indicated that on-plate enrichment can be used to enrich efficiently His_6 species from a small volume of sample (1 μL). Furthermore, the enrichment time was reduced to less than 1 min.

To demonstrate that our approach can be used to selectively enrich His-rich peptides such as His_6 from a complex peptide mixture, His_6 spiked in the tryptic digest of cytochrome *c* was used as the sample. Figure 3A shows the direct MALDI mass spectrum of the peptide mixture. In addition to the protonated His_6 pseudomolecular ion peak at m/z 841.3, the peaks at m/z 1168.7, 1434.9, 1562.9, and 1633.7 derived from the tryptic digest of cytochrome *c*, and the peak m/z 2163.0 derived from the self-digest of trypsin appeared in the same mass spectrum. After on-plate enrichment by the Fe_3O_4@Al_2O_3 MNPs, the peak at m/z 841.3 dominated the mass spectrum (Figure 3B).

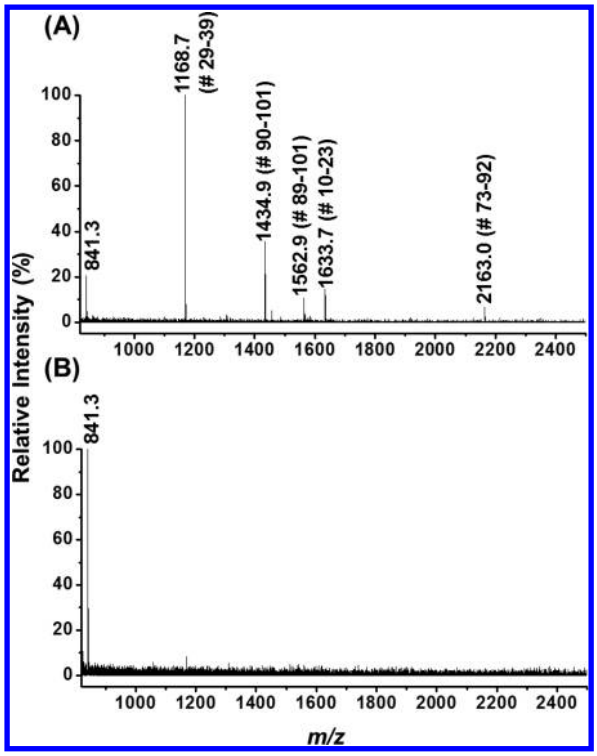

Figure 3. MALDI mass spectra of the tryptic digest of cytochrome *c* (3.3×10^{-6} M, 1 μL) containing His_6 (5×10^{-8} M, MH^+ = 841.3) obtained (A) before and (B) after on-plate enrichment by the Fe_3O_4@Al_2O_3 MNPs (1 μg).

The rest peaks were not observed in the same mass spectrum. The results demonstrated that the proposed platform can be used to efficiently enrich His-rich peptides from a complex peptide mixture.

The biomarker used for malaria diagnostics, i.e., HRP-II, contains multiple repeats of AHH and AHHAAD.[52] Thus, to further demonstrate the feasibility of using the current approach to enrich His-rich peptides from very complex samples, a His-rich peptide, i.e., AHHAHHAADAHHAH-HAAD (10 nM) spiked in 100-fold diluted human plasma by Tris buffer (pH 7), was used as a simulated sample. Figure 4A shows the direct MALDI mass spectrum of the 100-fold diluted human plasma spiked with the His-rich peptides. There are many peaks appearing in the low- and high-mass region. The peaks at m/z 16 573 (M^{4+}), 22 098 (M^{2+}), and 33 022 (M^{3+}) were presumably derived from multiply charged ions of human serum albumin since they are abundant in human plasma. Some low-mass peaks also appeared in the low-mass region (<10 000). Figure 4B shows the resultant mass spectrum obtained after using the Fe_3O_4@Al_2O_3 MNPs as affinity probes to selectively trap target species from the complex plasma sample spiked with AHHAHHAADAHHAHHAAD (MH^+ = 1915.0) on a MALDI plate. The peak at m/z 1915.0 dominated the mass spectrum, and the majority peaks appearing in Figure 4A disappeared. The results indicated that the current approach has the capability to selectively enrich trace amounts of His-rich peptides such as multiple repeats of AHH and AHHAAD from complex plasma samples. Thus, our approach may potentially be used in the rapid screening of the His-rich biomarkers from malaria-infected plasma samples.

One of the advantages of using the on-plate magnetic enrichment approach is the sample spots can be easily found

dx.doi.org/10.1021/ac4000128 | *Anal. Chem.* 2013, 85, 3347−3354

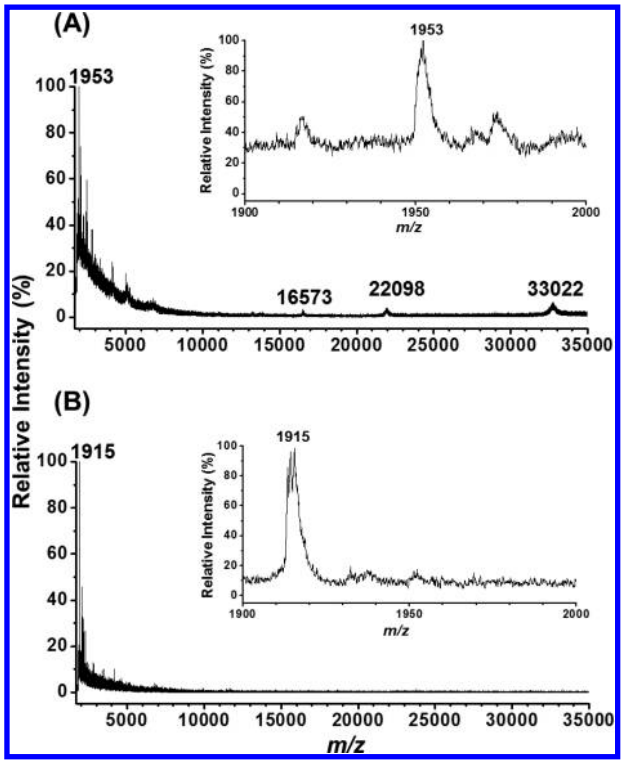

Figure 4. Direct MALDI mass spectrum of the 100-fold diluted human plasma (1 μL) spiked with AHHAHHAADAHHAHHAAD (10^{-8} M, MH^+ = 1915) obtained (A) before and (B) after on-plate enrichment by the Fe_3O_4@Al_2O_3 MNPs (1 μg).

from the magnetic aggregates when conducting MALDI-MS analysis. In particular, the "sweet spot" problem commonly encountered in MALDI-MS analysis became less serious. The target species were concentrated on a small spot; therefore, the analyte peak can be easily found, and the intensity of the target analyte can be greatly improved. Parts A and B of Figure 5

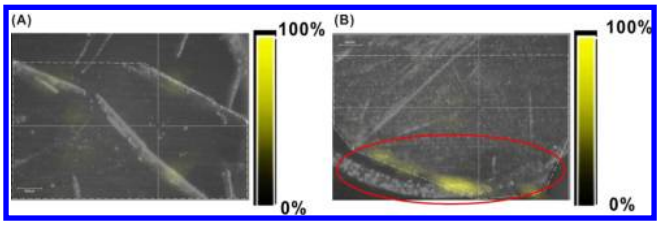

Figure 5. MALDI-MS images of the His_6 sample (5×10^{-8} M, 1 μL) at m/z 841 obtained (A) before enrichment and (B) after on-plate enrichment with Fe_3O_4@Al_2O_3 MNPs (1 μg). DHB (15 mg/mL) prepared in acetonitrile/deionized water (2:1, v/v) was used as the MALDI matrix.

show the MALDI images at m/z 841 derived from the protonated His_6 without and with on-plate magnetic enrichment of the sample (1 μL) containing His_6, respectively. Apparently, the ion peak at m/z 841 (marked with yellow) was randomly distributed with a low intensity in the sample well before the on-plate enrichment (Figure 5A), whereas the peak can be easily observed at an aggregated spot with a higher intensity after magnetic aggregation (Figure 5B). Given this behavior, the limit of detection for His_6 was obtained as low as ~0.4 nM (1 μL; Supporting Information Figure S4). We previously have used IMAC-based MNPs (Fe_3O_4@Ni(II)) as the enrichment probes for His_6 and conduced the enrichment by pipetting the MNPs/sample suspension (50 μL) in a centrifuge tube.[17] The limit of detection was estimated to be ~1 nM.[53] Thus, the results demonstrated that the current approach can provide better sensitivity than the previous MNP-based IMAC method. Furthermore, only a small amount (~1 μL) of sample required for conducting the analysis in the current approach.

Enzymatic protein digestion, combined with MS analysis and protein database search, is used for protein identification. We also performed on-plate tryptic digestion of the target proteins trapped by the Fe_3O_4@Al_2O_3 MNPs, followed by peptide enrichment. Figure 6A shows the direct MALDI mass spectrum

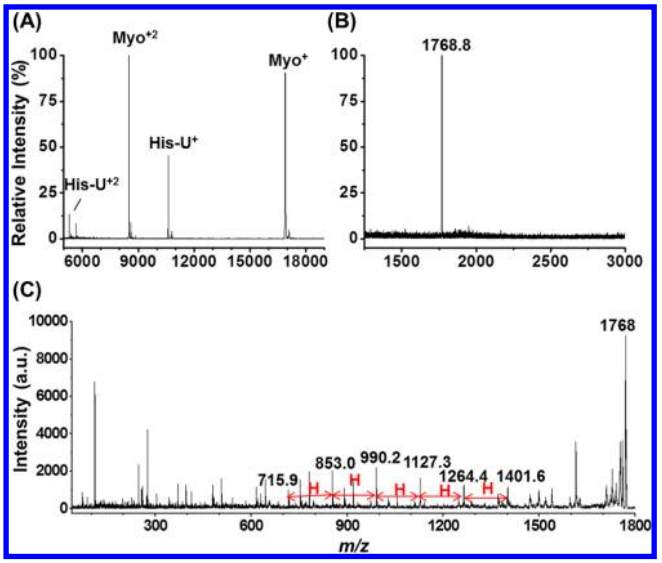

Figure 6. (A) Direct MALDI mass spectrum of a protein mixture (1.5 μL) of myoglobin (10^{-6} M) and His_6-tagged ubiquitin (10^{-6} M). (B) MALDI mass spectrum obtained after using Fe_3O_4@Al_2O_3 MNPs (3 μg) to enrich selectively the target species from the protein mixture (1.5 μL) of myoglobin (10^{-6} M) and His_6-tagged ubiquitin (10^{-6} M), conducting tryptic digestion for 5 min on the MALDI plate and then performing an on-plate enrichment. (C) MS/MS spectrum at m/z 1768.

of the protein mixture containing myoglobin (1 μM) and His_6-tagged ubiquitin (1 μM). The singly and doubly charged ions derived from myoglobin and His_6-tagged ubiquitin were observed in the mass spectrum. After the protein enrichment by the Fe_3O_4@Al_2O_3 MNPs (1 μg), tryptic digestion of the target proteins, and peptide enrichment from the tryptic digest by the same MNPs on the MALDI plate, only a peptide containing His_6 at m/z 1768.88 appeared in the MALDI mass spectrum (Figure 6B). The complete sequence of the His-tag ubiquitin is listed in the Supporting Information. The peak at m/z 1768.88 apparently represents the sequence GSSHHHHHHSSGLVPR (theoretical MH^+ = 1768.83). An MS/MS analysis at m/z 1768 was conducted to clarify whether the peak was derived from a His-rich peptide. Figure 6C shows the corresponding MS/MS spectrum. Several peaks were observed at m/z 1401.6, 1264.4, 1127.3, 990.2, 853.0, and 715.9 with a mass difference of ~137 between each pair of adjacent peaks, confirming that the peak at m/z 1768 is a His-rich peptide. Considering the loss of 137 stands for the loss of a His, the results indicated that the Fe_3O_4@Al_2O_3 MNPs have a desirable binding affinity with His-rich peptides.

dx.doi.org/10.1021/ac4000128 | Anal. Chem. 2013, 85, 3347−3354

E. coli BL21 was constructed to express His-tag fusion verotoxin type 2B. Thus, we used the cell lysate of *E. coli* BL21 that contained His-tag fusion verotoxin type 2B as the sample to demonstrate the feasibility of using our approach in real-world applications. Supporting Information Figure S5 displays the direct MALDI mass spectrum of the cell lysate of *E. coli* BL21. Only few ions at m/z 4768, 7319, and 9492 appeared in the mass spectrum. It is because urea was used as the cell lysis reagent, and its presence in the cell lysate sample caused poor matrix crystallization for undesirable MALDI results. Figure 7A

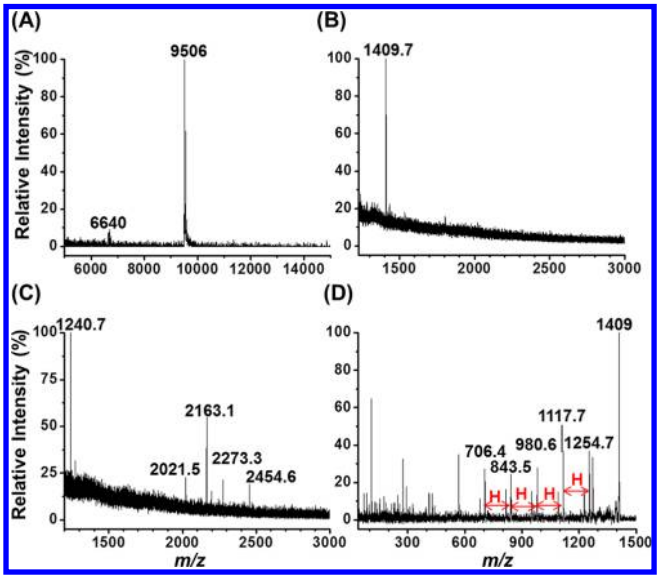

Figure 7. (A) MALDI mass spectrum obtained after using the Fe_3O_4@Al_2O_3 MNPs (3 μg) to enrich selectively the target species from *E. coli* BL21 cell lysate (1.5 μL) containing His-tag fusion verotoxin type 2B; (B) MALDI mass spectrum obtained by conducting an on-plate trypsin digestion of the protein trapped by the MNPs (panel A) and an on-plate peptide enrichment; (C) MALDI mass spectrum of the supernatant obtained after MNP enrichment on the plate. (D) MS/MS spectrum at m/z 1409.

displays the MALDI mass spectrum obtained after using the Fe_3O_4@Al_2O_3 MNPs to enrich the target species from the cell lysate selectively. Two new peaks at m/z 9506 and 6640 appeared in the mass spectrum, but the peaks observed in the mass spectrum in Supporting Information Figure S5 disappeared. The identities of these two peaks were unclear; thus, we further conducted an on-plate tryptic digestion followed by Fe_3O_4@Al_2O_3 MNPs enrichment. Figure 7B shows the resultant mass spectrum of the MNP−target species conjugates after on-plate enrichment. The peak at m/z 1409.7 dominated the mass spectrum. Figure 7C shows the MALDI mass spectrum of the supernatant after magnetic isolation. The peaks at m/z 1240.7, 2021.5, and 2454.6 were derived from the tryptic digest of Shiga-like toxin, and the peaks at m/z 2163.1 and 2273.3 were derived from the self-digestion product of trypsin (Supporting Information Table S1). These peaks were not His-rich peptides. An MS/MS analysis was conducted to clarify whether the peak was derived from a His-rich peptide. Several fragment peaks at m/z 1254.7, 1117.7, 980.6, 843.5, and 706.4 were observed, having a mass difference of ∼137 with adjacent peaks (Figure 7D). This result corresponded to the loss of a His. The results demonstrated that His-rich species from complex cell lysate samples can be rapidly confirmed by conducting these four steps: on-plate protein enrichment, tryptic digestion, peptide enrichment, and then followed by MALDI-MS characterization.

Fe_3O_4@Al_2O_3 MNPs have been used in the enrichment of phosphorylated species as mentioned earlier.[30,31,33−35] The selectivity of the MNPs toward His-rich species in the presence of phosphorylated species is worth investigating. Thus, we used a mixture of His_6−ubiquitin and β-casein as the model sample to examine the selectivity of the MNPs toward His-rich proteins by conducting these three steps: enrichment, tryptic digestion, and enrichment of target species by the Fe_3O_4@Al_2O_3 MNPs on plate at pH 7. Parts A and B of Figure 8 show

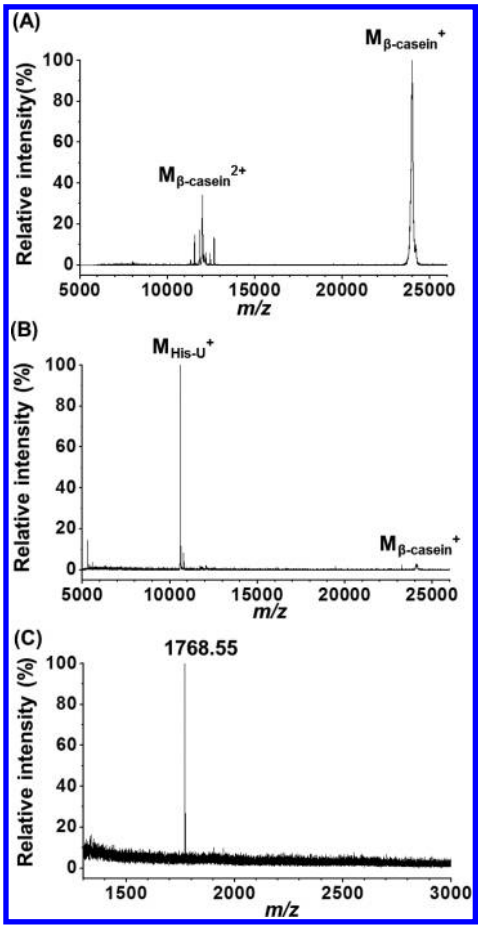

Figure 8. (A) Direct MALDI mass spectrum of the protein mixture containing His_6-tagged ubiquitin (5×10^{-7} M) and β-casein (5×10^{-5} M); (B) MALDI mass spectrum obtained after using the Fe_3O_4@Al_2O_3 MNPs as the affinity probes to enrich selectively the target species from the same sample (1 μL) as used for panel A; (C) MALDI mass spectrum obtained after conducting on-plate tryptic digestion of the target species enriched by the Fe_3O_4@Al_2O_3 MNPs from the sample used in panel B.

the resultant MALDI mass spectra obtained before and after the on-plate enrichment of the target protein, respectively. Only two peaks derived from the doubly ($M_{\beta\text{-casein}}^{2+}$) and singly charged ions ($M_{\beta\text{-casein}}^{+}$) of β-casein appeared in the mass spectrum before the enrichment because the concentration of His-tagged ubiquitin was 100 times lower than that of β-casein. However, after on-plate enrichment, the peak exhibited by the His_6-tagged ubiquitin ($M_{His\text{-}U}^{+}$) dominated the mass spectrum (Figure 8B), which further showed only a low-intensity peak of $M_{\beta\text{-casein}}^{+}$. The results indicated that the selectivity of the MNPs toward His_6-tagged ubiquitin is significantly better than that of

dx.doi.org/10.1021/ac4000128 | *Anal. Chem.* 2013, 85, 3347−3354

β-casein. We further conducted on-plate tryptic digestion followed by on-plate peptide enrichment. Figure 8C shows that only a peak at m/z 1768.55 appeared in the mass spectrum. The peak seemed to be a His-rich peptide. MS/MS was used to confirm the identities, which revealed similar results to that in Figure 6C, thus confirming that the peak at m/z 1768.55 was derived from a His-rich peptide. The results indicated that the Fe_3O_4@Al_2O_3 MNPs have better selectivity for His-rich species than phosphorylated species at pH 7.

CONCLUSIONS

In this study, we successfully demonstrated that Fe_3O_4@Al_2O_3 MNPs have good binding selectivity toward His-rich peptides/proteins. As the results demonstrated here, the sensitivity of our approach is better than the previous MNP-based IMAC approach. The binding affinity of the current approach for poly-His is comparable with Cu(II)-IMAC, but it is worse than Ni(II)-IMAC in terms of the estimation of the binding constant. When on-plate magnetic enrichment is combined with tryptic digestion, followed by MALDI-MS analysis, His-rich species can be quickly characterized within 10 min. Considering that the analysis was conducted on a MALDI plate, 1−2 μL of sample is already sufficient for the analysis. This platform is particularly suitable in quickly checking whether His_6 fusion proteins have been expressed in cultured cells. Additionally, the approach may be potentially suitable in rapidly screening the presence of a malaria biomarker in biological fluids since we have demonstrated the feasibility of using the current approach to rapidly enrich trace amount of His-rich peptides containing multiple repeats of AHH and AHHAAD from complex plasma sample. Although Fe_3O_4@Al_2O_3 MNPs are good affinity probes for phosphorylated species, enrichment of phosphorylated species is usually conducted in acidic solutions. As demonstrated in this study, the best pH condition for the enrichment of His-rich species by the Fe_3O_4@Al_2O_3 MNPs is at pH 7; the binding affinity of Fe_3O_4@Al_2O_3 MNPs for poly-His at acidic conditions is quite poor. Thus, by manipulating the pH in sample solutions, Fe_3O_4@Al_2O_3 MNPs can be used to enrich His-rich or phosphorylated species from complex samples selectively. This characteristic makes Fe_3O_4@Al_2O_3 MNPs a good choice for complex samples containing both His-rich species and phosphorylated molecules. Additionally, it should be noticed that this approach is suitable for trace analysis and quick examination of the presence of target analytes. Nevertheless, conventional column-based MOAC approach is a better choice when preparative-scale purification is anticipated.

ASSOCIATED CONTENT

Supporting Information

Additional information as noted in text. This material is available free of charge via the Internet at http://pubs.acs.org.

AUTHOR INFORMATION

Corresponding Author

*E-mail: yuchie@mail.nct.edu.tw. Fax: +886-3-5723764.

Notes

The authors declare no competing financial interest.

ACKNOWLEDGMENTS

We thank the National Science Council of Taiwan for financial support. We also thank Professor Hiroshi Morie, who provided us *E. coli* BL21.

REFERENCES

(1) Parra, M. E.; Evans, C. B.; Taylor, D. W. *J. Clin. Microbiol.* **1991**, *29*, 1629−1634.
(2) de Souza Castilho, M.; Laube, T.; Yamanaka, H.; Alegret, S.; Pividori, M. I. *Anal. Chem.* **2011**, *83*, 5570−5577.
(3) Hengen, P. *Trends Biochem. Sci.* **1995**, *20*, 285−286.
(4) Porath, J.; Carlsson, J.; Olsson, I.; Belfrage, G. *Nature* **1975**, *258*, 598−599.
(5) Posewitz, M. C.; Tempst, P. *Anal. Chem.* **1999**, *71*, 1883−1892.
(6) Stensballe, A.; Andersen, S.; Jensen, O. N. *Proteomics* **2001**, *1*, 207−222.
(7) Gaberc-Porekar, V.; Menart, V. *J. Biochem. Biophys. Methods* **2001**, *49*, 335−360.
(8) Raska, C. S.; Parker, C. E.; Dominski, A.; Marzluff, W. F.; Glish, G. L.; Pope, R. M.; Borchers, C. H. *Anal. Chem.* **2002**, *74*, 3429−3433.
(9) Block, H.; Maertens, B.; Spriestersbach, A.; Brinker, N.; Kubicek, J.; Fabis, R.; Labahn, J.; Schäfer, F. *Methods Enzymol.* **2009**, *463*, 439−472.
(10) Zhou, W.; Merrick, B. A.; Khaledi, M. G.; Tomer, K. B. *J. Am. Soc. Mass Spectrom.* **2000**, *11*, 273−282.
(11) Hart, S. R.; Waterfield, M. D.; Burlingame, A. L.; Cramer, R. *J. Am. Soc. Mass Spectrom.* **2002**, *13*, 1042−1051.
(12) Thompson, A. J.; Hart, S. R.; Franz, C.; Barnouin, K.; Ridley, A.; Cramer, R. *Anal. Chem.* **2003**, *75*, 3232−3243.
(13) Stensballe, A.; Jensen, O. N. *Rapid Commun. Mass Spectrom.* **2004**, *18*, 1721−1730.
(14) Liu, H.; Stupak, J.; Zhang, J.; Keller, B. O.; Brix, B. J.; Fliegel, L.; Li, L. *Anal. Chem.* **2004**, *76*, 4223−4232.
(15) Hirschberg, D.; Jägerbrink, T.; Samskog, J.; Gustafsson, M.; Stählberg, M.; Alveliusm, G.; Husman, B.; Carlquist, M.; Jörnvall, H.; Bergman, T. *Anal. Chem.* **2004**, *76*, 5864−5871.
(16) Dunn, J. D.; Watson, J. T.; Bruening, M. L. *Anal. Chem.* **2006**, *78*, 1574−1580.
(17) Li, Y.-C.; Lin, Y.-S.; Tsai, P.-J.; Chen, C.-T.; Chen, W.-Y.; Chen, Y.-C. *Anal. Chem.* **2007**, *79*, 7519−7525.
(18) Liu, S.; Chen, H.; Lu, X.; Deng, C.; Zhang, X.; Yang, P. *Angew. Chem., Int. Ed.* **2010**, *49*, 7557−7561.
(19) Maa, Z.; Guana, Y.; Liua, H. *J. Magn. Magn. Mater.* **2006**, *301*, 469−477.
(20) Xu, C.; Xu, K.; Gu, H.; Zhong, X.; Guo, Z.; Zheng, R.; Zhang, X.; Xu, B. *J. Am. Chem. Soc.* **2004**, *126*, 3392−3393.
(21) Xu, C.; Xu, K.; Gu, H.; Zheng, R.; Liu, H.; Zhang, X.; Guo, Z.; Xu, B. *J. Am. Chem. Soc.* **2004**, *126*, 9938−9939.
(22) Pinkse, M. W. H.; Uitto, P. M.; Hilhorst, M. J.; Ooms, B.; Heck, A. J. R. *Anal. Chem.* **2004**, *76*, 3935−3943.
(23) Gaberc-Porekar, V.; Menart, V. *Chem. Eng. Technol.* **2005**, *28*, 1306−1314.
(24) Kweon, H. K.; Hakansson, K. *Anal. Chem.* **2006**, *78*, 1743−1749.
(25) Wolschin, F.; Wienkoop, S.; Weckwerth, W. *Proteomics* **2005**, *5*, 4389−4397.
(26) Ficarro, S. B.; Parikh, J.; Blank, N. C.; Marto, J. A. *Anal. Chem.* **2008**, *80*, 4606−4613.
(27) Dunn, J. D.; Reid, G. E.; Bruening, M. L. *Mass Spectrom. Rev.* **2010**, *29*, 29−54.
(28) Chen, C.-T.; Chen, Y.-C. *Anal. Chem.* **2005**, *77*, 5912−5919.
(29) Lo, C.-Y.; Chen, W.-Y.; Chen, C.-T.; Chen, Y.-C. *J. Proteome Res.* **2007**, *6*, 887−893.
(30) Chen, C.-T.; Chen, C.-T.; Tsai, P.-J.; Chien, K.-Y.; Yu, J.-S.; Chen, Y.-C. *J. Proteome Res.* **2007**, *6*, 316−325.
(31) Liu, J.-C.; Tsai, P.-J.; Lee, Y. C.; Chen, Y.-C. *Anal. Chem.* **2008**, *80*, 5425−5432.

(32) Chen, C.-T.; Chen, Y.-C. *J. Biomed. Nanotechnol.* **2008**, *4*, 73−79.
(33) Li, Y.; Liu, Y.; Tang, J.; Lin, H.; Yao, N.; Shen, X.; Deng, C.; Yang, P.; Zhang, X. *J. Chromatogr., A* **2007**, *1172*, 57−71.
(34) Chen, C.-T.; Chen, Y.-C. *J. Mass Spectrom.* **2008**, *43*, 538−541.
(35) Yu, T.-J.; Li, P.-H.; Tseng, T.-W; Chen, Y.-C. *Nanomedicine* **2011**, *6*, 1353−1363.
(36) Chen, W.-Y.; Chen, Y.-C. *Anal. Bioanal. Chem.* **2010**, *398*, 2049−2057.
(37) Lin, H.-Y.; Chen, W.-Y.; Chen, Y.-C. *J. Biomed. Nanotechnol.* **2009**, *5*, 215−223.
(38) Zeng, Y. Y.; Chen, H. J.; Shiau, K. J.; Hung, S. U.; Wang, Y. S.; Wu, C. C. *Proteomics* **2012**, *1*, 380−390.
(39) Hoang, T.; Roth, U.; Kowalewski, K.; Belisle, C.; Steinert, K.; Karas, M. *Anal. Chem.* **2010**, *82*, 219−228.
(40) Joshi, S.; Ghosh, I.; Pokhrel, S.; Madler, L.; Nau, W. M. *ACS Nano* **2012**, *6*, 5668−5679.
(41) Lin, J.-Y.; Chen, Y.-C. *Talanta* **2011**, *86*, 200−207.
(42) Porath, J. *Protein Express. Purif.* **1992**, *3*, 263−281.
(43) Suen, S.-Y.; Liu, Y.-C.; Chang, C.-S. *J. Chromatogr., B* **2003**, *797*, 305−319.
(44) Pearson, R. G. *J. Am. Chem. Soc.* **1963**, *85*, 3533−3539.
(45) Chen, C.-T. Doctoral Dissertation, National Chiao Tung University, Hsinchu, Taiwan, 2008.
(46) Tsuji, T.; Shimizu, T.; Sasaki, K.; Shimizu, Y.; Tsukamoto, K.; Arimitsu, H.; Ochi, S.; Sugiyama, S.; Taniguchi, K.; Neri, P.; Morie, H. *Vaccine* **2008**, *26*, 469−476.
(47) Chen, W.-Y.; Chen, Y.-C. *Anal. Bioanal. Chem.* **2006**, *386*, 699−704.
(48) Tulej, M.; Riedo, A.; Iakovleva, M.; Wurz, P.; *Int. J. Spectrosc.* **2012**, *2012*, Article ID 234949.
(49) Dall'Osto, M.; Harrison, R. M.; Highwood, E. J.; O'Dowd, C.; Ceburnis, D.; Querol, X.; Achterberg, E. P. *Atmos. Environ.* **2010**, *44*, 3135−3146.
(50) Grams, J. *New Trends and Potentialities of TOF-SIMS in Surface Studies*; Nova Science Publishers: New York, 2007.
(51) Nieba, L.; Nieba-Axamann, S. E.; Persson, A.; Hamalainen, M.; Edebratt, F.; Hansson, A.; Lidholm, J.; Magnusson, K.; Karlsson, A. F.; Pluckthun, A. *Anal. Biochem.* **1997**, *252*, 217−228.
(52) Panton, L. J.; McPhie, P.; Maloy, W. L.; Wellems, T. E.; Taylor, D. W.; Howard, R. J. *Mol. Biochem. Parasitol.* **1989**, *35*, 149−160.
(53) Li, Y.-C. Master's Dissertation, National Chiao Tung University, Taiwan, 2006.